

# Dynamic assessment of spontaneous baroreflex sensitivity by means of time–frequency analysis using either RR or pulse interval variability

Michele Orini, Luca T. Mainardi, Eduardo Gil, Pablo Laguna and Raquel Bailón

**Abstract**—In this study we propose a method to continuously assess the changes of spontaneous baroreflex sensitivity (BRS). Systolic arterial pressure and RR intervals are analyzed by time–frequency analysis to estimate their instantaneous powers as well as the time–course of their spectral coherence. The BRS estimated in classical frequency bands is compared to the BRS estimated in dynamic frequency bands centered on respiratory frequency. The possibility of obtaining reliable estimations of the BRS using the pulse interval from the pressure signal as a surrogate of the RR is considered. Results on a tilt table test database suggest that is possible to obtain reliable BRS estimates just from the analysis of the pressure signal, without the need of ECG recordings.

## I. INTRODUCTION

The baroreflex is one of the homeostatic mechanism for maintaining blood pressure. The assessment of baroreflex sensitivity [1] (BRS, i.e. the change in the RR interval following a unitary change in the blood pressure) from non-invasive measurements is challenging since a baroreflex impairment has been suggested to have diagnostic and prognostic relevance. In the last 20 years different techniques have been proposed to estimate the spontaneous BRS [2]. Among them there is the simultaneous analysis of systolic arterial pressure variability (SAPV) and RR variability (RRV) in the frequency domain, via spectral analysis. In particular, the parameter  $\alpha$  has been defined as the squared root of the ratio between the power content of RRV and SAPV [2], and it is usually defined in the LF and HF bands. This parameter is computed whenever the linear coupling between SAPV and RRV, assessed through spectral coherence estimation, is higher than an arbitrary threshold. The modulus of the spectral coherence usually presents two peaks, one centered around typical Mayer wave frequency (about 0.1 Hz) and an other centered around respiratory frequency. Thus, the respiratory rate should be taken into account in the analysis of the BRS. Most of the autonomic tests used to evoke a cardiovascular response, such as tilt table test, Valsalva maneuver, exercise stress testing etc. are non-stationary. In such situations the interest lies in the dynamic assessment of the BRS and time–frequency (TF) analysis is required. Among the different TF and time–varying methods which

have been applied to the study of the cardiovascular variability [3], the smoothed pseudo Wigner–Ville distribution (SPWVD) is one of the most interesting, since it provides an independent control of time and frequency resolution. Recently, a method to robustly estimate the TF coherence between cardiovascular variables, based on the SPWVD, has been presented [4]. The time–varying quantification of the linear coupling between RRV and SAPV through TF coherence analysis allows to define time epochs during which reliable estimates of  $\alpha(t)$  can be obtained. Finally, one limitation of the spontaneous BRS analysis is that it requires the simultaneous recording of the ECG and the pressure signal. Thus, the aims of this study are: (1) present a comprehensive framework for the continuous estimation of  $\alpha(t)$  in non-stationary conditions based on the SPWVD; (2) discuss the importance of including the respiratory rate in the analysis of the BRS and (3) assess the possibility of estimating  $\alpha(t)$  without the need of the ECG recordings, i.e. using the pulse interval variability estimated from the pulse waves in the pressure signal as an alternative measurement of the RR variability.

## II. METHODS

### A. Signal acquisition and preprocessing

Thirteen young volunteers (age  $28.2 \pm 2.7$  years, 9 males) without any previous cardiovascular history underwent a head–up tilt table test without fainting. In this test, subjects undergo a progressive orthostatic stress and blood pressure is maintained thanks to baroreflex regulation [5], which involves an increase in heart rate and a constriction of the blood vessels in the legs. The experimental protocol consisted of: 3 minutes in early supine position ( $T_1$ ), 5 minutes tilted head–up to an angle of  $70^\circ$  ( $T_2$ ) and 3 minutes back to later supine position ( $T_3$ ). The ECG and respiratory signals were recorded using the Biopac MP 150 system with a sampling frequency of 1 kHz and 125 Hz, respectively, while the pressure signal was recorded using the Finometer system with a sampling frequency of 250 Hz. Beats from ECG and pulses from the pressure signal were detected to generate RR, pulse interval and systolic arterial pressure time series. During the procedure, the device used for pressure signal recording was recalibrated at the beginning of  $T_2$  and  $T_3$ . The recalibration took few seconds and introduced artefacts which were detected and corrected by interpolation. All the time series were subsequently resampled at 4 Hz and RR variability (RRV), pulse interval variability (PIV) and systolic arterial pressure variability (SAPV) were obtained

This work was supported by Ministerio de Ciencia y Tecnología, FEDER under Project TEC2007-68076-C02-02/TCM; and by the Centro de Investigación Biomédica en Red de Bioingeniería, Biomateriales y Nanomedicina (CIBER–BBN) through Instituto de Salud Carlos III (ISCIII);

M. Orini, R. Bailón, E. Gil and P. Laguna are with the Technology Communication Group, i3A, University of Zaragoza, 50018 Zaragoza, Spain; and also with CIBER–BBN, Spain; [michele@unizar.es](mailto:michele@unizar.es)

M. Orini and L.T. Mainardi are with Department of Bioengineering, Politecnico di Milano, Milan, Italy.

by high-pass filtering the corresponding series with a cut-off frequency of 0.03 Hz.

### B. Time-frequency analysis

The smoothed pseudo Wigner-Ville distribution (SPWVD) was used to estimate the time-varying spectral properties of the cardiovascular variables, as well as to perform TF coherence analysis. The cross-SPWVD is defined as [6]:

$$S_{x,y}(t, f) = \int_{-\infty}^{\infty} \int_{-\infty}^{\infty} \phi(\tau, \nu) A_{x,y}(\tau, \nu) e^{j2\pi(\nu - f)\tau} d\nu d\tau \quad (1)$$

$$A_{x,y}(\tau, \nu) = \int_{-\infty}^{\infty} a_x\left(t + \frac{\tau}{2}\right) a_y^*\left(t - \frac{\tau}{2}\right) e^{-j2\pi\nu t} dt \quad (2)$$

where  $a_x(t)$  and  $a_y(t)$  are the complex analytic signal representations of the original real signals  $\{x, y\} \in \{\text{RRV, PIV, SAPV}\}$ ;  $A_{x,y}(\tau, \nu)$  is the narrowband symmetric ambiguity function (AF) of  $a_x(t)$  and  $a_y(t)$  and can be seen as the 2D Fourier transform of the Wigner-Ville distribution. The kernel  $\phi(\tau, \nu)$  is a 2D weighting function which performs the TF low-pass filtering necessary to suppress the interference terms which reduce the readability of the Wigner-Ville distribution. The SPWVD of signal  $x(t)$  is obtained using  $y = x$ . We choose as kernel the elliptical exponential function previously used to obtain a robust estimation of the TF coherence [4]:

$$\phi(\tau, \nu; \tau_0, \nu_0) = \exp\left\{-\pi \left[\left(\frac{\nu}{\nu_0}\right)^2 + \left(\frac{\tau}{\tau_0}\right)^2\right]^{\frac{1}{2}}\right\} \quad (3)$$

The kernel's iso-contours are ellipses whose major axis length, i.e. the bandwidth of the TF low-pass filter, depends on parameters  $\tau_0$  and  $\nu_0$ . Parameters  $\tau_0$  and  $\nu_0$  were selected to have a frequency resolution of 0.031 Hz and a time resolution of 15 s. These values corresponded to the full width at half maximum of the Fourier transform of  $\phi(\tau, 0)$  and  $\phi(0, \nu)$ , respectively. Time-frequency coherence, used to continuously quantify the strength of the linear coupling between pairs of signals during time, was then estimated as [7], [4]:

$$\gamma_{x,y}(t, f) = \sqrt{\frac{S_{x,y}(t, f) S_{x,y}^*(t, f)}{S_x(t, f) S_y(t, f)}}. \quad (4)$$

### C. Spectral band definition and indices estimation

Respiration affects RRV, through respiratory sinus arrhythmia (RSA), and SAPV, through mechanical changes provoked in the intra-thoracic pressure and vessel compliance. Thus, the inclusion of the respiratory rate  $F_R(t)$  in the analysis can improve the estimation of spectral RRV and SAPV indices [8] and could help to interpret the results. To evaluate the effect of including (or not) the respiratory rate in the BRS analysis, two kinds of spectral bands were defined. Instantaneous powers as well as instantaneous band coherences were then estimated by integrating  $S_x(t, f)$  and averaging  $\gamma_{x,y}(t, f)$  in these spectral bands, defined as:

I) Time-invariant traditional bands (TI-B); TI-LF  $\in [0.04, 0.15]$  Hz and TI-HF  $\in [0.15, 0.4]$  Hz were used for the estimation of instantaneous powers  $P_{\text{TI-B}}^x(t)$  and band coherence  $\gamma_{\text{TI-B}}^{x,y}(t)$ , with  $\text{TI-B} \in \{\text{TI-LF, TI-HF}\}$ ;

II) Time-varying respiration-dependent bands (TV-B); Two dynamic frequency ranges were defined, the TV-RSA and the TV-LF bands. For instantaneous power estimation, TV-RSA band was dynamically centered around  $F_R(t)$  while TV-LF band was centered around the instantaneous frequency  $F_{\text{LF}}^x(t)$ , estimated as the maximum of  $S_x(t, f)$  in traditional TI-LF band. Both bands were twice the frequency resolution wide (0.062 Hz), unless TV-RSA and TV-LF bands overlapped. In this case the upper limit of TV-LF band decreased to the lower limit of TV-RSA band. In those cases in which the width of TV-LF band was lower than the frequency resolution (i.e.  $F_R(t) - F_{\text{LF}}^x(t) < 0.031$ ), estimation of  $P_{\text{TV-LF}}^x(t)$  was discarded. For band coherence estimation, we used the same TV-RSA as for power estimation, whereas TV-LF band was centered around  $(F_{\text{LF}}^x(t) + F_{\text{LF}}^y(t))/2$  and the same rules mentioned above were adopted for its dynamic adjustment. When TV respiration-dependent bands were used, instantaneous powers and band coherences were noted as  $P_{\text{TV-B}}^x(t)$  and  $\gamma_{\text{TV-B}}^{x,y}(t)$ , with  $\text{TV-B} \in \{\text{TV-LF, TV-RSA}\}$ . The respiratory rate  $F_R(t)$  was estimated as the maximum of the SPWVD of the respiratory signal in a frequency range from 0.04 to 0.5 Hz and was carefully revised to avoid misestimations due to movement artefacts. The time-course of the BRS was then estimated as:

$$\alpha_{\text{TI-B}}^{x,y}(t) = \sqrt{\frac{P_{\text{TI-B}}^x(t)}{P_{\text{TI-B}}^y(t)}}; \quad \alpha_{\text{TV-B}}^{x,y}(t) = \sqrt{\frac{P_{\text{TV-B}}^x(t)}{P_{\text{TV-B}}^y(t)}}; \quad (5)$$

with  $x \in \{\text{RRV, PIV}\}$  and  $y \in \{\text{SAPV}\}$ . Instantaneous estimations of  $\alpha(t)$  were accepted only for those  $t$  for which band coherences were higher than 0.5 and discarded otherwise. The Wilcoxon test was applied for every  $t$  to statistically compare the instantaneous values of  $P_B^x(t)$ ,  $\gamma_B^{x,y}(t)$  and  $\alpha_B^{x,y}(t)$  to baseline values (obtained by averaging  $P_B^x(t)$ ,  $\gamma_B^{x,y}(t)$  and  $\alpha_B^{x,y}(t)$  in  $T_1$ ). The percentage of total time during which differences were statistically significant ( $T_{\%}$ ) as well as the mean  $p$ -value ( $\bar{p}$ ) obtained in those epochs were then estimated in  $T_2$  and  $T_3$ . The first 40 s of  $T_2$  and  $T_3$  were excluded to discard the effect of artefacts due to recalibration.

## III. RESULTS

In our study population,  $F_R(t)$  presented high inter-subject variability. In only 6 subjects the TV-RSA band never overlapped with TI-LF band, while in 5 subjects the TV-RSA band overlapped with the TI-LF band and reduced the width of the TV-LF band to less than the frequency resolution for almost the entire recording (>90%). In these 5 subjects  $P_{\text{TV-LF}}^x(t)$  and  $\gamma_{\text{TV-LF}}^{x,y}(t)$  were not estimated.

In Fig. 1, we report the averaged time-courses of indices  $P_B^{\text{RRV}}(t)$  and  $P_B^{\text{PIV}}(t)$  (panels (a)-(b)),  $P_B^{\text{SAPV}}(t)$  (panels (c)-(d)),  $\gamma_B^{x,y}(t)$  (panels (e)-(f)) and  $\alpha_B^{x,y}(t)$  (panels (g)-(h)) for both types of spectral bands TI-B (left panels) and TV-B (right panels). Results obtained using PIV instead of RRV are reported in dotted lines. Black crosses mark the presence of artefacts in the pressure signal. In Fig. 2, results are given as the temporal mean and standard deviation of the cardiovascular indices, averaged among subjects. Results of the statistical analysis are shown in table I only for those

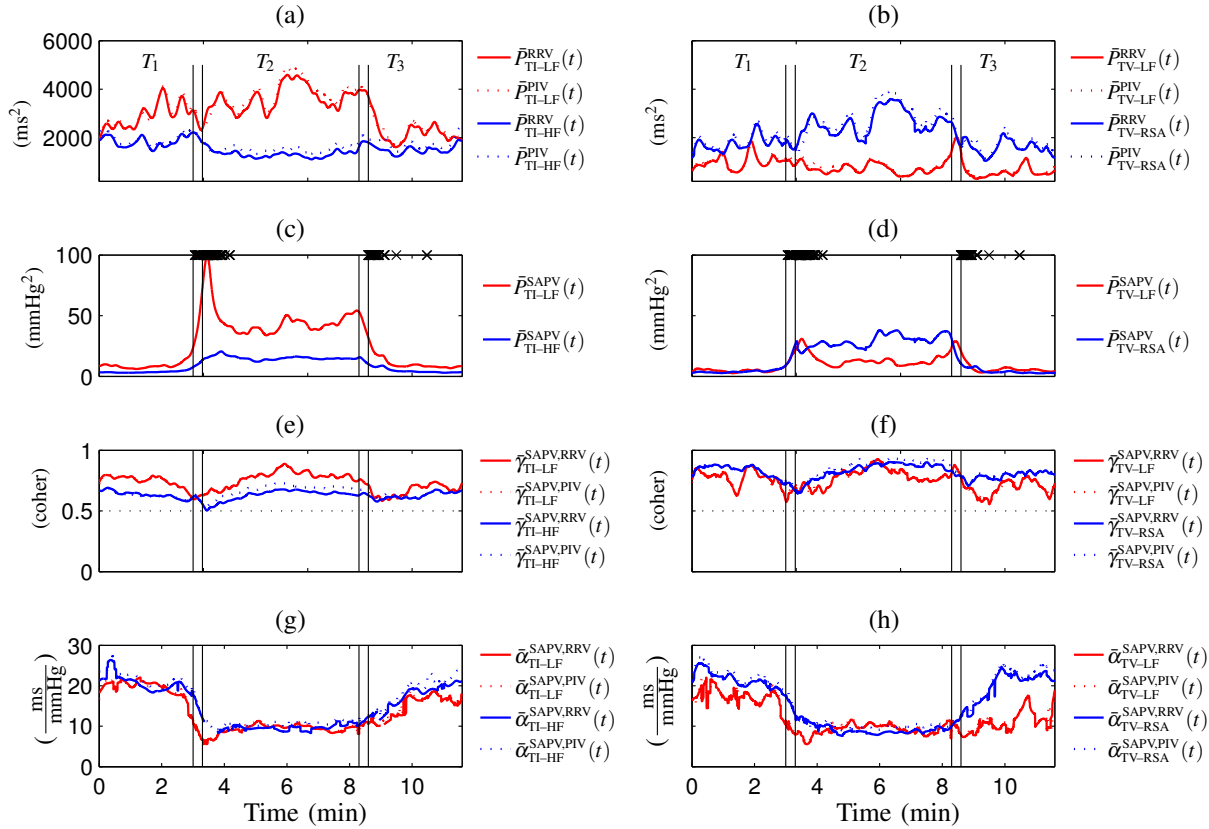


Fig. 1. Mean time-course of cardiovascular indices. Left and right panels refers to estimations obtained using time-invariant and time-varying respiration-dependent bands, respectively; LF and HF values are in red and blue lines, respectively; estimations obtained using the PIV as a surrogate of RRV are in dotted lines.

indices whose time-course significantly changed with respect to baseline. Panels 1(a)–(d) show that using different types of spectral bands, i.e. TI-B or TV-B, we obtained different results. By using TI-B, we observed that  $P_{\text{TI-LF}}^x(t) > P_{\text{TI-HF}}^x(t)$ , for both RRV and SAPV, whereas the use of TV-B led to opposite results. As shown in table I, the increase of  $P_{\text{B}}^{\text{SAPV}}(t)$  in  $T_2$  was statistically significant in TI-LF, TI-HF and TV-RSA, while it was almost never significant in TV-LF band. This difference is likely due to the inclusion or not in the statistical analysis of those 5 subjects for whom the TV-RSA band overlapped with the TI-LF band for almost the entire recording. Moreover, excluding them from the statistical analysis performed on results obtained using TI-B, the increase of  $P_{\text{TI-B}}^{\text{SAPV}}(t)$  in  $T_2$  became not significant in TI-LF ( $T_{\%} = 1\%$ ) and less significant in TI-HF ( $T_{\%} = 27\%$ ). From panels 1(e)–(f) we observe that the averaged time-courses of  $\gamma_{\text{TI-LF}}^{x,\text{SAPV}}(t)$  and  $\gamma_{\text{TV-LF}}^{x,\text{SAPV}}(t)$ , with  $x \in \{\text{RRV}, \text{PIV}\}$ , was high during the entire procedure and slightly decreased at the beginning of  $T_2$  and  $T_3$ , probably due to the presence of artefacts in the pressure signal. The averaged time-course of  $\gamma_{\text{TV-RSA}}^{\text{RRV},\text{SAPV}}(t)$  was also very high, while the lower value of  $\gamma_{\text{TI-HF}}^{\text{RRV},\text{SAPV}}(t)$  was likely due to the fact that, in several subjects, the central frequency of the spectral component related to respiration moved into TI-LF. Interestingly, the differences in the estimates obtained with different spectral bands slightly affected the estimation of the BRS. Indeed, as shown in Fig. 1 and 2, similar

results were obtained for  $\alpha_{\text{B}}^{x,y}(t)$  using both TV-B and TI-B. The increase of  $P_{\text{B}}^{\text{SAPV}}(t)$  during head-up tilt, made  $\alpha_{\text{B}}^{x,y}(t)$  decrease in all spectral bands. This decrease was always significant ( $T_{\%} = 100\%$ ,  $\bar{p} < 0.007$ ) except during TV-LF. Finally, from Fig. 1 and 2 and table I, we observed that the use of the PIV signal instead of the RRV signal did not produce any relevant effect in LF band. In TI-HF and TV-RSA,  $P_{\text{B}}^{\text{RRV}}(t) < P_{\text{B}}^{\text{PIV}}(t)$  and  $\gamma_{\text{B}}^{\text{RRV},\text{SAPV}}(t) < \gamma_{\text{B}}^{\text{PIV},\text{SAPV}}(t)$ , with  $\text{B} \in \{\text{TI-HF}, \text{TV-RSA}\}$ . However, these differences were small and even further decreased in the estimation of parameter  $\alpha_{\text{B}}^{x,y}(t)$ . For example, as shown in Fig. 2, during  $T_2$  difference between mean values of  $\alpha_{\text{B}}^{\text{RRV},\text{SAPV}}(t)$  and  $\alpha_{\text{B}}^{\text{PIV},\text{SAPV}}(t)$  were lower than 0.4 ms/mmHg for TI-LF and TV-LF and lower than 1.1 ms/mmHg for TI-HF and TV-RSA.

#### IV. DISCUSSION

In this study we presented a framework to continuously quantify the baroreflex sensitivity based on TF analysis. The SPWVD was used to perform TF and TF coherence analysis of RRV, PIV and SAPV. The degree of TF filtering gives a good TF resolution while providing consistent estimations of TF coherence ( $\gamma_{x,y}(t, f) \in [0, 1] \forall$  subjects). A time-varying estimation of band coherence, necessary to accept the estimation of  $\alpha_{\text{B}}^{x,y}(t)$ , is obtained by averaging  $\gamma_{x,y}(t, f)$  in the spectral bands. As for spectral coherence,  $\gamma_{x,y}(t, f)$  is affected by the parameters used in its calculation, i.e.

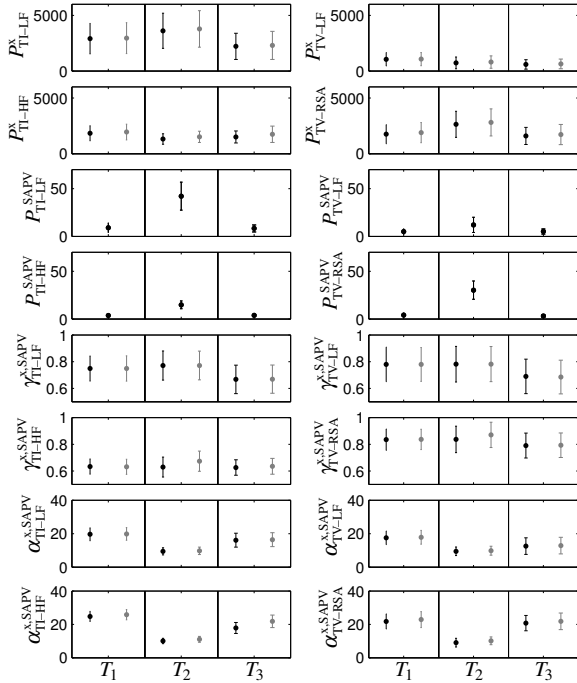


Fig. 2. Averaged of temporal mean and SD among subjects. Left panels: TI-B. Right panels: TV-B. Black and grey colors indicate that values were obtained using  $x$ =RRV and  $x$ =PIV, respectively.

TABLE I

STATISTICAL ANALYSIS TO ASSESS THE CHANGES IN  $T_2$  WITH RESPECT TO BASELINE ( $T_1$ )

	$T_2$	$T_2$
	$T_{\%} (\bar{p})$	$T_{\%} (\bar{p})$
$P^{SAPV}_{TI-LF}$	77 (2e-2)	$P^{SAPV}_{TV-LF}$ 7 (4e-2)
$P^{SAPV}_{TI-HF}$	100 (2e-3)	$P^{SAPV}_{TV-RSA}$ 82 (3e-2)
$\alpha^{RRV,SAPV}_{TI-LF}$	100 (6e-3)	$\alpha^{RRV,SAPV}_{TV-LF}$ 38 (3e-2)
$\alpha^{RRV,SAPV}_{TI-HF}$	100 (4e-3)	$\alpha^{RRV,SAPV}_{TV-RSA}$ 100 (2e-3)
$\alpha^{PIV,SAPV}_{TI-LF}$	100 (7e-3)	$\alpha^{PIV,SAPV}_{TV-LF}$ 39 (3e-2)
$\alpha^{PIV,SAPV}_{TI-HF}$	100 (2e-3)	$\alpha^{PIV,SAPV}_{TV-RSA}$ 100 (2e-3)

by the degree of TF smoothing performed by  $\phi(\tau, \nu)$ . To reduce the dependence of band coherence on the degree of TF smoothing, we used TV spectral bands whose width depended on the TF resolution. This justified the use of  $\gamma_{xy}(t, f)$ , which is characterized by the same TF resolution as the TF spectra, instead of the quadratic TF coherence as proposed elsewhere [2]. Time–frequency analysis allows to track the changes of the autonomic modulation of heart rate and arterial pressure and to continuously assess the strength of their linear coupling in different spectral ranges of interest. The assessment of the dynamics of the baroreflex sensitivity by means of the SPWVD is appealing due to its good TF resolution and robustness. Nevertheless, a limitation compared to causal autoregressive model–based methodologies [9] is the impossibility to disentangle the feedback baroreflex mechanism (from SAPV to RRV) from other mechanisms (mechanical feedforward mechanism from

RRV to SAP, cardio–pulmonary reflex, etc) [10]. Moreover, the simultaneous estimation of the respiratory rate allows one to interpret the changes observed in the cardiovascular indices in relation with the respiration. Indeed, we showed that, when respiratory–rate is low, the increase of the power of the RRV and SAPV signals observed in TI–LF band during head–up tilt could be enhanced by the interactions between the respiratory–driven oscillations and the baroreflex regulation activity around 0.1 Hz. Nevertheless, the parameter  $\alpha(t)$ , which significantly decreased in response to the orthostatic stress provoked by head–up tilt, only slightly changed by using different spectral bands. The similarity between  $\alpha^{xy}_{TI-LF}(t)$  and  $\alpha^{xy}_{TV-LF}(t)$  and between  $\alpha^{xy}_{TI-HF}(t)$  and  $\alpha^{xy}_{TV-RSA}(t)$  can be justified considering that the BRS were estimated only in those TF regions where the coupling between RRV and SAPV was consider sufficiently high. An important finding of this study is that PIV estimated from the pressure signal may be used as a surrogate of RRV in the BRS analysis. Indeed, indices estimated using PIV instead of RRV presented the same temporal pattern (Fig. 1) with mean differences lower than their mean standard deviations (Fig. 2) and led to very similar results when a statistical test is performed (table I). If this finding is confirmed on larger study populations it would give the opportunity to obtain reliable estimates of BRS without the need of the ECG recordings, i.e. only using the pressure signal from the finger.

## REFERENCES

- [1] M. Di Rienzo, G. Parati, A. Radaelli, and P. Castiglioni, “Baroreflex contribution to blood pressure and heart rate oscillations: time scales, time-variant characteristics and nonlinearities,” *Phil Trans R Soc A*, vol. 367, no. 1892, pp. 1301–1318, Apr. 2009.
- [2] D. Laude, *et al.*, “Comparison of various techniques used to estimate spontaneous baroreflex sensitivity (the eurobarvar study).” *Am J Physiol Regul Integr Comp Physiol*, vol. 286, no. 1, pp. R226–R231, Jan 2004.
- [3] L. T. Mainardi, “On the quantification of heart rate variability spectral parameters using time-frequency and time-varying methods,” *Phil Trans R Soc A*, vol. 367, no. 1887, pp. 255–275, Jan 28 2009.
- [4] M. Orini, R. Bailón, L. Mainardi, A. Mincholé, and P. Laguna, “Continuous quantification of spectral coherence using quadratic time-frequency distributions: error analysis and application,” *Internat. Conf. Computers in Cardiology*, pp. 681–684, 2009.
- [5] P. O. O. Julu, V. L. Cooper, S. Hansen, and R. Hainsworth, “Cardiovascular regulation in the period preceding vasovagal syncope in conscious humans.” *J Physiol*, vol. 549, no. 1, pp. 299–311, May 2003.
- [6] F. Hlawatsch, “Duality and classification of bilinear time-frequency signal representations,” *IEEE Trans. Signal Processing*, vol. 39, no. 7, pp. 1564–1574, July 1991.
- [7] G. Matz and F. Hlawatsch, “Time-frequency coherence analysis of nonstationary random processes,” in *Proc. Tenth IEEE Workshop Statistical Signal and Array Processing*, 2000, pp. 554–558.
- [8] R. Bailón, P. Laguna, L. Mainardi, and L. Sornmo, “Analysis of heart rate variability using time-varying frequency bands based on respiratory frequency,” in *Proc. 29th Annual Int Conf IEEE-EMBS 2007*, 22–26 Aug. 2007, pp. 6674–6677.
- [9] H. Zhao, W. A. Cupples, K. H. Ju, and K. H. Chon, “Time-varying causal coherence function and its application to renal blood pressure and blood flow data,” *IEEE Trans Biomed Eng*, vol. 54, no. 12, pp. 2142–2150, Dec. 2007.
- [10] A. Porta, *et al.*, “Quantifying the strength of the linear causal coupling in closed loop interacting cardiovascular variability signals.” *Biol Cybern*, vol. 86, no. 3, pp. 241–251, Mar 2002.